 THIS PROJECT HAS RECEIVED FUNDING FROM THE FUEL CELLS AND HYDROGEN 2 JOINT UNDERTAKING (JU) UNDER GRANT AGREEMENT NO 101007170. THE JU RECEIVES SUPPORT FROM THE EUROPEAN UNION'S HORIZON 2020 RESEARCH AND INNOVATION PROGRAMME AND HYDROGEN EUROPE AND HYDROGEN EUROPE RESEARCH.

Material, Operating strategy and REliability optimisation for
LIFEtime improvements in heavy duty trucks

D3.2 CCM with two commercial membranes and two catalyst types prepared

Public

DOCUMENT INFORMATION

Project	**MORELife**
Grant Agreement No.	**N° 101007170**
Deliverable No.	**D3.2**
Deliverable Title	**CCM with two commercial membranes and two catalyst types prepared**
Dissemination Level	**PU**
Nature	**R**
Deliverable Version	**V1.0**
Deliverable Date	**2022-02-02**
Deliverable Responsible	**Dr. Stanko Hočevar**

AUTHORS/REVIEWERS TABLE

	Author(s) / Organization	**Date**
Written by	**Dr. Stanko Hočevar, Jernej Hočevar /Mebius d.o.o.**	**2022-01-20**
Reviewed by	**Dr. Antoni Forner-Cuenca / TU/e**	**2022-01-28**
Approved by	**Coordinator / AVL**	**2022-02-01**

CHANGE HISTORY

Version	**Who**	**Description**	**Date**
V0.1	**Dr. Stanko Hočevar**		**2022-01-20**
V0.2	**Dr. Stanko Hočevar**	**Corrected after review**	**2022-01-31**
V1.0	**Hermine Pirker**	**Released version by coordinator after Formatting Corrections**	**2022-02-02**

Contents

List of Figures

List of Tables

1 Publishable Executive Summary

In T3.2 to which this report on D3.2 belongs, Mebius has modified the original ORR catalyst, delivered to TUM for analyses and MEA preparations for single cell tests and AST (see D3.1 report), by subsurface doping of catalyst nanoparticles with non-metal element to enhance the catalyst activity and durability.

Further on, Mebius has prepared an optimised catalyst ink and used it to prepare CCMs with commercial ePTFE Nafion membrane.

The CCMs and MEAs prepared with these CCMs were delivered to project partners for single cell tests and AST.

2 Deviations from original Description in the Grant Agreement Annex 1 Part A

2.1 Description of work related to deliverable in GA Annex 1 – Part A

original Text from GA – Annex 1 –Part A
Optimised catalyst ink formulation suitable for inkjet printing (ink composition, I/C ratio, viscosity, surface tension) of the modified cathode catalysts synthesised in T3.1 will be defined, and the catalysts will be inkjet printed on cathode side of two types of commercial membranes: SSC PFSA and e-PTFE reinforced PFSA. The Pt loading on cathode side will be 0.25 mg_{Pt}/cm^2_{geom}. For anode side commercial Pt/C catalyst will be used with Pt loading of 0.1 mg_{Pt}/cm^2_{geom}.

2.2 Time deviations from original planning in GA Annex 1 – Part A

There are no deviations with respect to timing of this deliverable.

2.3 Content deviations from original plan in GA Annex 1 – Part A

There are no deviations from the Annex 1 – Part A with respect to the content.

3 Introduction

The second phase of the project is focused on advancing and improving MEA materials to compensate for the anticipated failure modes determined in the initial phase (WP2) and to improve the material utilisation to meet the cost and loading targets (i.e. 0.3 g/kW). Overall, within the project, improved materials and operating strategies are selectively optimised though experience and field data to balance the PGM loading with the application target requirements for performance, cost, and lifetime. Specifically, this is achieved using MEBs innovative, proprietary ORR catalyst that enables lower PGM content, higher mass activity and higher durability compared to conventional commercial ORR catalysts. The technology of catalyst synthesis is at TRL3. MEBs innovative ORR catalyst will be combined with SoA membranes, specifically selected based on the HD requirements, that provide with high conductivity and superior durability. Further, MEB holds an innovative technology for catalyst ink deposition that offers a high degree of flexibility regarding the MEA geometry, PGM loading, ionomer content, and constituent distributions (graded CLs). The technology of catalyst ink deposition is at TRL4. MEB thus produces catalyst coated membrane (CCM) based MEAs using Freudenberg GDL+MPL, with active areas between 5 and 50 cm^2 for small-active-area single cell and 5-cell stack tests at project partners. The technology of CCM MEA preparation is at TRL4. MEB will also test in-house prepared 25 cm^2 MEAs at the facilities of JRC Petten during the approved open call project MEBIUSMEA. This will serve as a method of down-selection, as only suitable materials will be further tested in NFCT and EKPO industrial hardware in a short stack (≥10-cell or 1 kW) configuration. As leaching of catalyst core compounds is identified as a potential concern for lifetime with core-shell structured catalysts, special attention is devoted to this. A risk with these new materials arises when the core metals are exposed during load-cycling and then dissolve into the ionomer phase. This process can lead to additional MEA degradation via catalyst deactivation mechanisms.

4 Technical Section

4.1 Strategy for improvement of proprietary catalyst activity and durability

As we stated in the D3.1 report, where we described the performance of the initial Mebius ORR catalyst delivered to TUM for electrochemical and physico-chemical characterization, the catalyst has lower than needed performance in single cell tests at high current densities. In the conclusions of that report, we also stated that "the challenge of achieving high current densities, however, remains to be solved. It is very likely that in the present catalyst the main obstacle is the oxygen mass transport in the microporous carbon support, as indirectly confirmed by the analysis of polarization curves with the Kulikovsky model. As a consequence, the cell voltage at power density of 791 mW cm^{-2} and current density of 1.5 A cm^{-2} is 0.532 V. This is about 130 mV lower than the targeted performance. Further optimization of the catalyst synthesis parameters, pre-treatment, and MEA production is underway".

Our initial catalyst has two main deficiencies:

- too broad nanoparticles size distribution, which reflects in low ESA values
- high content of Cu in the Cu_3Pt nanoparticles, which reflects in high concentration of leached-out Cu^{2+} ions from nanoparticles into the ionomer membrane causing degradation of membrane and Cu deposition on the Pt of the anode catalyst.

In accordance with the description of WP3 we have studied numerous possible approaches described in the recent open literature to improve our catalyst performance. We have identified two approaches that we are pursuing in phase 2 of the project.

To narrow the catalyst nanoparticle size distribution and anchor the nanoparticles stronger to the carbon support, we shall use HSA carbons modified (doped) by S and/or N. The recent excellent publication of Yang C-L. and co-authors [1] gives overwhelming evidence that the use of S-doped carbon support in intermetallic catalyst synthesis results in nanoparticles smaller than 5 nm with very high specific and mass activity and higher durability than SoA ORR catalysts. Strong interaction between platinum and sulfur suppresses metal sintering up to 1000°C. They have synthesized intermetallic libraries of small nanoparticles consisting of 46 combinations of platinum with 16 other metal elements and used them to study the dependence of electrocatalytic oxygen-reduction reaction activity on alloy composition and platinum skin strain. The intermetallic libraries are highly mass efficient in proton-exchange-membrane fuel cells and could achieve high activities of 1.3 to 1.8 amperes per milligram of platinum at 0.9 volts.

The application of Pt alloy catalysts for oxygen reduction reactions (ORRs) in proton-exchange membrane fuel cells is severely impeded by base metal leaching, since the produced metal ions can result in the degradation of a Nafion membrane by replacing H^+ and inducing a Fenton reaction. This is the second most challenging problem to be solved on the way to produce durable and active ORR catalysts. Recently, Lu B-A. and co-authors developed a catalyst nanoparticles phosphorus-doping strategy, which can greatly boost the ORR performance of Pt [2]. They have introduced phosphorus into the near-surface of commercial Pt/C catalyst via a surfactant-free method. This phosphorus-doping strategy is also valid for a Pt transition metal alloy catalysts to further boost the activity and durability in ORR.

In the WP3, T3.2 we have prepared the proprietary $PtCu_3$/C catalyst with phosphorus introduced into the near surface of the catalyst nanoparticles to enhance the durability and activity of the catalyst. With this modified catalyst we are preparing the first inkjet printed CCMs with 12 µm thick ePTFE reinforced Nafion membrane (Gore-Select Membrane M788.12) that will be delivered to partners for single cell testing.

4.2 Basics of inkjet printing

The material deposition inkjet printing technology is a well-established mass production technology in different technology fields: electronic devices, OLED production, etc.

In the case of electrocatalyst deposition either on proton exchange membranes to form catalyst coated membrane (CCM) or on the gas diffusion layer with microporous layer to form gas diffusion electrode (GDE), the inkjet printing technology is still in the development phase. This is mainly for two reasons: the development of adequately designed printheads and proper catalyst ink formulation. It is worth mentioning that each new catalyst type requires the development of appropriate ink. We have a 10-year of experience in depositing catalysts by inkjet printing technology on different substrates.

There are only a few printhead designs suitable for printing catalyst dispersion inks since the main ink ingredient, graphitised carbon, agglomerates with a particle size distribution from submicron to several microns dimension. The upper limit of particle size must be 10 to 20 times smaller than the nozzle aperture of the printhead to print the ink without nozzle clogging.

The ink formulation regulates the drop formation at the printhead nozzle. Drop behaviour can be represented as a "phase diagram" in a parameter space bound by the dimensionless number Z (the inverse of the Ohnesorge number) and the Weber number of the fluid jet before drop formation, W_{ej}. Stable drop generation is found to be bounded by a parallelogram with minimum and maximum values of $2 < W_{ej} < 25$ and minimum and maximum values of $2 < Z < 20$. To fit the ink inside these boundaries, one must optimise the values of surface tension, density, and dynamic viscosity of the ink.

Inkjet printers consist of basic three parts: the motion stage, the vision system, and the control systems including the print heads. The nozzle heads are directly connected to a reservoir or cartridge containing the ink, and the pressure control system applies pneumatic force (pulse train) not only to push the ink to the head, but also to define the ink meniscus at the nozzle orifice. Inkjet printing systems typically require three mechanical degrees of freedom, two translational (X and Y stages) and one rotational (Θ stage) to create 2D patterns and align with previously printed patterns to realize facilely stacked structures, respectively. A vision system consisting of at least two cameras is also necessary to enable substrate alignment (fiducial camera) and to observe ejected droplets in flight (drop-watching camera) to obtain well-defined droplets. Control systems are employed to optimize the temperature of both the stage and the nozzle, which can directly affect the substrate temperature and the dropping velocity, respectively (scheme of a piezoelectric type of inkjet-printer is shown in Figure 4.1-1).

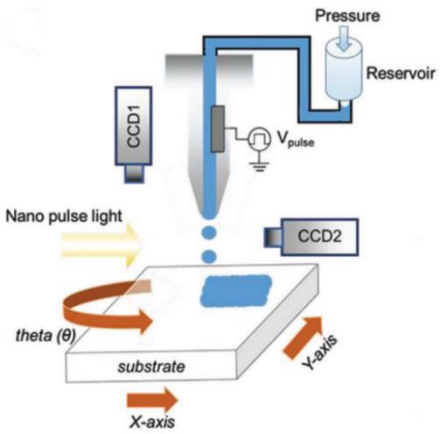

Figure 4-1: Scheme of a piezoelectric type of inkjet-printer

The ejected droplet formation mechanism is largely classified into two systems using 1) thermal nozzles and 2) piezoelectric nozzles. Thermal nozzles employ a heater in the form of a resistor. If the internal temperature is enough to create a bubble in a reservoir by increasing current, it facilitates the single droplet formation of ink out of the nozzle via volume expansion. Then, the negative pressure, forming inside the reservoir after the droplet has been ejected, draws new ink inside the reservoir. To utilize thermal nozzles to create droplets, the inks must be heat-compatible and sensitive to the volume contraction/expansion depending on the temperature. By contrast, piezoelectric nozzles contain a piezoelectric film placed along the wall of a reservoir, so the deformation of the film drives the mechanical volume expansion by applying voltage pulses. Then, the ink can be ejected in response to the pressure generated by the piezoelectric element. Therefore, piezoelectric nozzles with relatively better resolution, requiring lower temperature, and enabling more precise operation are preferred for realizing printed devices that do not suffer from ink degradation concerns and temperature-sensitive solvent choice, although thermal nozzles are typically less expensive and widely used in commercial printers. Note that the droplet size and velocity in flight are dominantly determined by the diameters of nozzles and maximum voltage of the input pulse train (Figure 4.1-2).

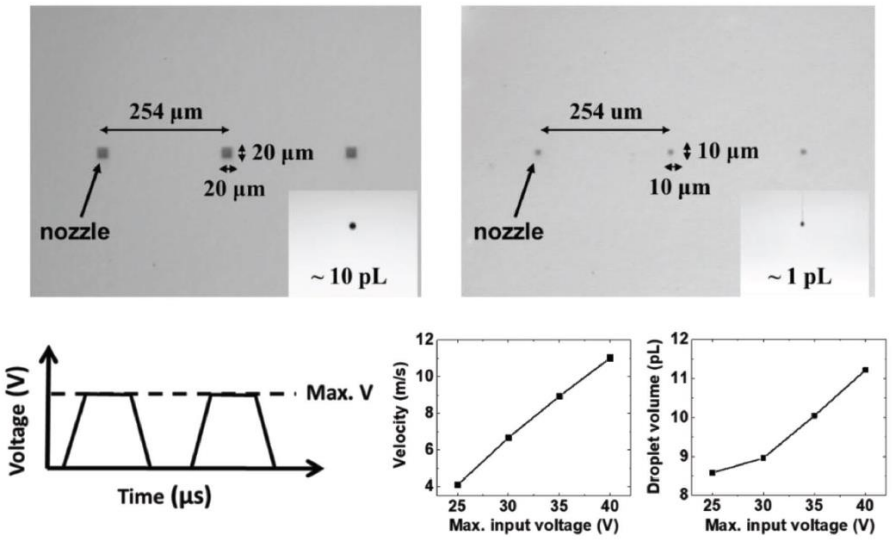

Figure 4-2: Influence of the diameter of nozzles and maximum voltage of the input pulse train on the droplet velocity and size.

Therefore, we will describe inkjet printing focusing on a piezoelectric type with drop-on-demand (DOD) characteristics, which we are using in our MEAs production process.

Stable drop formation without satellite droplets after ejection from the nozzles is also important to obtain well-defined printed patterns on a substrate. This behaviour closely incorporates the transfer of kinetic energy from the nozzles to the ejected droplets. In the initial state, the ink in the nozzle is in equilibrium. Upon applying a voltage pulse signal into the piezoelectric element, the ink extrudes out due to the volume expansion inside the nozzle. After kinetic energy over a threshold is transferred to the extruded ink, an in-flight droplet is generated and then drops toward the target substrate. In the sequentially applied opposite voltage, the ink in the nozzles refills, and the process repeats. In DOD inkjet printing, a droplet is generated by separation from the ink inside the nozzle when the piezoelectric element is actuated. This behaviour

means that an idle state, i.e., nonjetting condition, applies a small voltage pulse to the nozzle during the nonjetting condition to avoid ink drying and nozzle clogging.

The other fluid properties that should be considered for creating well-defined droplets are ink viscosity, surface tension, density, and inertia. In particular, surface tension and viscosity are the primary physical properties that determine the shape and droplet-tail of in-flight droplets, and satellite droplet formation.

For further normalized analysis, the primary four dimensionless numbers, the Reynolds number (*Re*), the Weber number (*We*), the capillary number (*Ca*), and the Ohnesorge number (*Oh*), are calculated as follows:

$$Re = \frac{inertial\ force}{viscous\ force} = \frac{\rho d v}{\eta} \quad (1)$$

$$We = \frac{inertial\ force}{surface\ tension\ force} = \frac{\rho v^2 d}{\gamma} \quad (2)$$

$$Ca = \frac{viscous\ force}{surface\ tension\ force} = \frac{\eta v}{\gamma} \quad (3)$$

$$Oh = \frac{\sqrt{We}}{Re} = \frac{\eta}{\sqrt{\gamma \rho d}} \quad (4)$$

where ρ is the ink density, d is the nozzle diameter, v is the velocity of the ink, η is the viscosity of the ink, and γ is the surface tension. These dimensionless parameters offer a window of jetting conditions for general inks regardless of composition. For example, if the jetting is dominated by a high-viscosity ink, a large value of *Oh* (>1) is extracted, whereas unstable jetting can be observed if *Oh* has a small value (<0.1). In other words, the Ohnesorge number actually describes the compatibility ("ink printability") between the ink chosen for the printing process (hence its dependence on γ, ρ, and η) and the equipment used for droplets generation (hence its dependence on *d*). It should be noted that the inverse Ohnesorge number ($Z = Oh^{-1}$) is also widely used ($1 < Z < 10$). *Ca* is typically determined by the diameter of the nozzle and does not depend on the characteristic length. In commercial inkjet printing systems, typical nozzle diameters are in the range of 20–60 µm, a tolerable ink viscosity range is 0.5–40 cP and a tolerable surface tension range is 20–70 dyne cm^{-1} [3].

The printability of an ink suitable for use with an inkjet printer is defined by the ability to eject a well-formed single drop without the formation of satellite drops. A parameter space defined by the dimensionless parameters Z and W_{ej} can best determine the printability of a fluid with known (Newtonian) physical properties. The use of Z is justified because it does not contain a velocity term. The Weber number is determined using the velocity of the fluid prior to drop formation, i.e. the fluid jet Weber number, W_{ej}. This more accurately captures the mechanisms of drop ejection and gives a fairer representation of the practical utility of an ink. The region of printability is bounded by maximum and minimum values of W_{ej} ($2 < W_{ej} < 25$) and is shaped in the fashion of a parallelogram, centred around $Z \approx 2–20$, with different behaviour at low and high values of Z (see Figure 4.1-3).

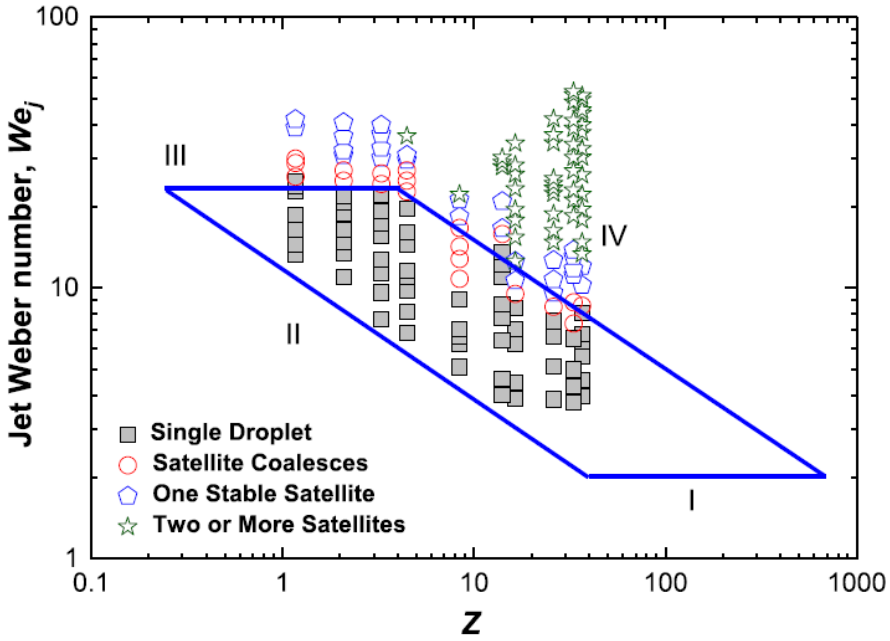

Figure 4-3: Phase diagram for printability in a parameter space of Z and the jet Weber number, Wej. Filled symbols indicating stable single drop generation at lower values of Wej and a sequence of satellite drops forming above an upper threshold value of Wej. Superimposed upon the experimental data is a parallelogram representing the inferred regime of fluid printability, which indicates 4 transition regimes labeled I–IV [4].

The lower bound of W_{ej} = 2 represents the limiting capillarity forces that must be overcome for drop formation (bound I). The upper bound of W_{ej} = 25 represents the intrinsic instability of the extended tail that forms as a drop is ejected (bound III). The low Z limit to printability (bound II) indicates a region where viscous forces become increasingly important and the minimum W_{ej} for drop ejection increases with decreasing Z, accompanied by an increase in the minimum actuation voltage for drop ejection. At large Z, the maximum W_{ej} before satellites form decreases with increasing Z because the low viscosity fluid forms liquid columns that readily pinch off to form satellites (bound IV). However, at both high and low values of Z, the range of fluid velocities (W_{ej}) between the minimum value for drop ejection and the onset for satellite formation is small, and thus the practical range for ink printability is approximately bound by $2 < Z < 20$. [Liu Y, 2019]

4.3 Description of the inkjet printer used for CCM MEA preparation

Mebius uses the FUJIFILM Dimatix Materials Printer DMP – 2831 with Dimatix Materials Cartridges Model # DMC – 11610

System description:

- Flat substrate, xyz stage, “ink jet” deposition system
- Low cost, user-fillable piezo-based ink jet print cartridges
- Built-in drop jetting observation system
- Fiducial camera for substrate alignment and measurement
- Variable jetting resolution and pattern creation PC-controlled with Graphical User Interface (GUI) application software

- Capable of jetting a wide range of fluids
- Heated vacuum platen
- Cartridge cleaning station
- Includes PC, monitor, and software

Mechanical System

- Printable area

- Substrate < 0.5 mm thickness: 210 mm x 315 mm (8.27 in x 12.4 in)
- Substrate 0.5 - 25 mm thickness: 210 mm x 260 mm (8.27 in x 10.2 in)

- Repeatability: ± 25 µm (± 0.001 in)
- Substrate holder

- Vacuum platen
- Temperature adjustable; ambient to 60° C

- System Footprint: 673 mm x 584 mm x 419 mm (26 in x 23 in x 16 in)
- Weight approximately 43 kg (95 lbs)
- Power 100-120/200-240 VAC 50/60 Hz 375 W maximum
- Operating range 15-40° C at 5-80% RH non-condensing
- Altitude up to 2000 m
- Safety and EMC compliance

- Safety: NRTL Certified to EN 61010-1, UL 61010-1, CSA 22.2 No. 61010-1
- EMC: EN61326-1 Class A, FCC Part 15 Class A

Fiducial Camera

- Allows substrate alignment using reference marks
- Allows positioning a print origin or reference point to match substrate placement
- Provides measurement of features and locations
- Provides inspection and image capture of printed pattern or drops
- Provides cartridge alignment when using multiple cartridges
- Allows matching drop placement to previously patterned substrate

Cartridge

- Type: Piezo-driven jetting device with integrated reservoir and heater
- Usable Ink Capacity: Up to 1.5 ml (user-fillable)
- Materials Compatibility: Many water-based, solvent, acidic or basic fluids
- Number of Nozzles: 16 nozzles, 254 µm spacing, single row
- Drop Volume: 1 (DMC-11601) and 10 (DMC-11610) picoliter nominal

Control PC and Application Software

- Pre-loaded patterned templates
- Pattern preview
- Editors: Pattern, piezo drive waveform, cleaning cycle, substrate setting

- Bitmap (1 bit) files accepted
- DXF, Gerber, GDSII and OASIS file conversion to Bitmap

Replaceable Items

- Print cartridge with one-time
- user-fillable reservoir
- Cleaning station nozzle blotting pad
- Drop watcher fluid absorbing pad.

4.4 Ink formulation for Mebius proprietary catalyst and preparation for printing

4.4.1 Catalyst ink composition

The catalyst ink is composed of:

- Proprietary catalyst Pt-Cu/C with 33.4 wt.% total metal loading on Vulcan XC72R carbon support (Cabot, Italy)
- Solvent 2-Propanol (Merck KGaA, Germany), MilliQ water
- Nafion® solution D1021 (Ion Power, GmbH, Germany)

4.4.2 Catalyst ink preparation for printing

- The ink components were added in suitable proportion and in the correct sequence to form a suspension
- The suspension was sonified in an ultrasound bath (Elmasonic P, Elma Schmidbauer GmbH, Germany) for a minimum of 1 hour
- Visual inspection after sonification for sedimentation at the bottom of the container
- If no sediment is visible the ink is ready for printing, otherwise continue sonification.

4.4.3 Printing parameters

- Printing pattern drop spacing 25 µm
- Printhead sabre angle minimum 5.6 degrees
- To ensure correct drop formation on the printhead the printing waveform has to be adjusted to the physical properties of the ink
- To ensure uninterrupted printing one must follow the instuctions in the manual by using the Drop Watcher module to determine the maximum jetting frequency of the fluid.

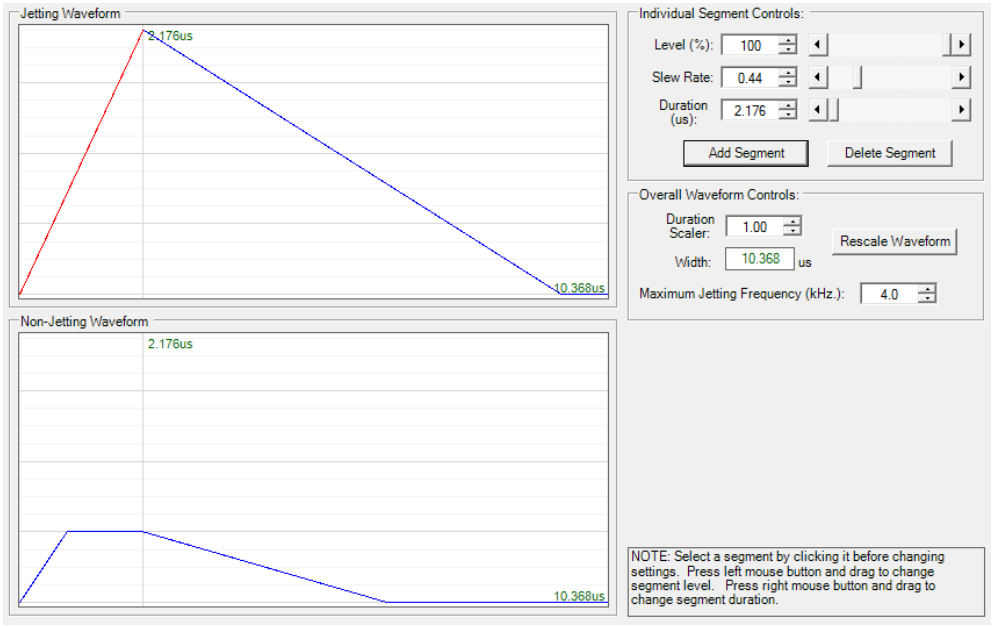

Figure 4-4: The wave form applied for inkjet printing the Mebius catalyst ink (courtesy of Mebius d.o.o.)

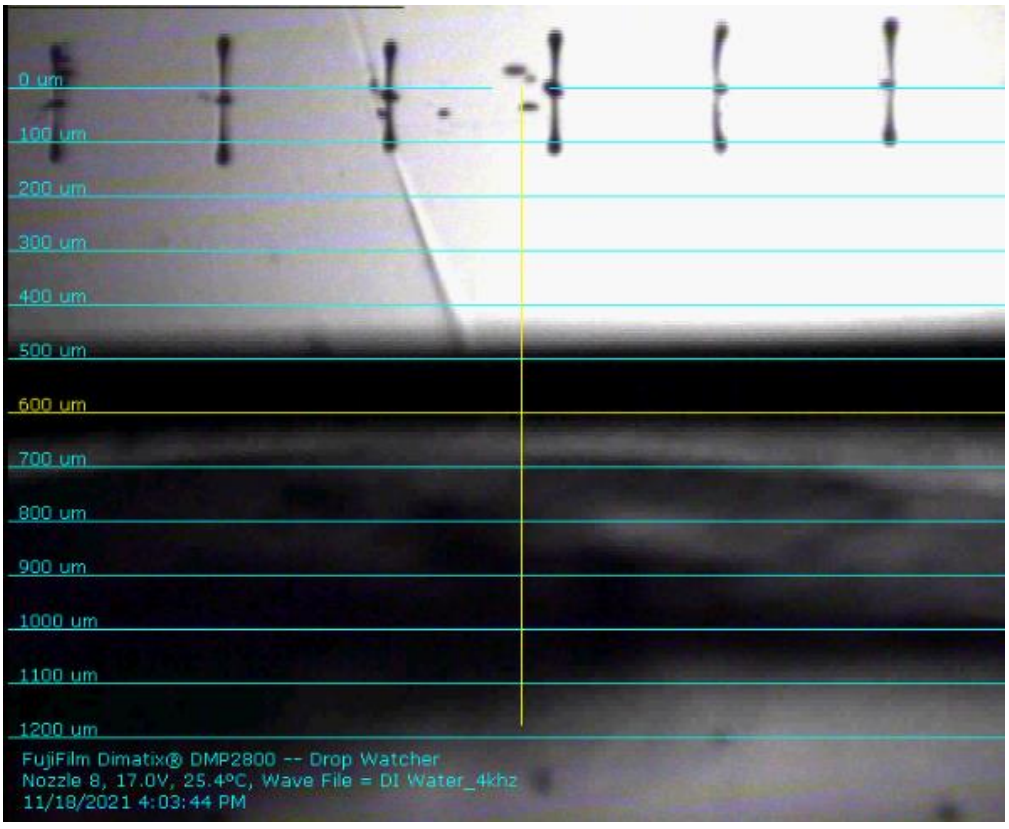

Figure 4-5: Catalyst ink – formation of drops scanned by Dropwatcher camera of the printer (courtesy of Mebius d.o.o.)

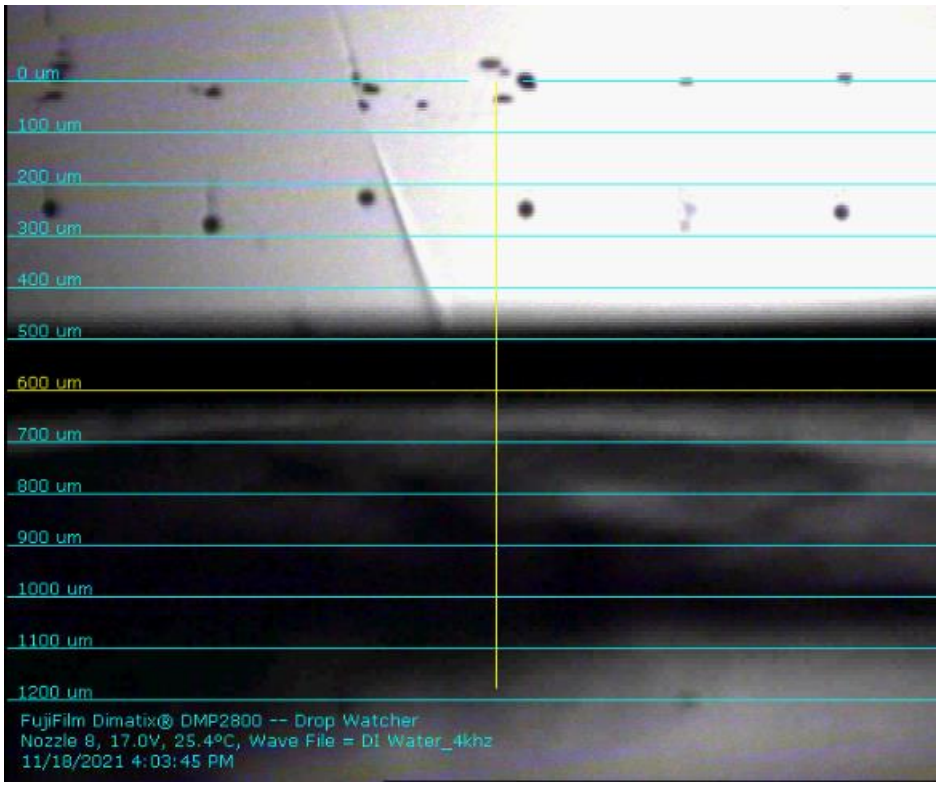

Figure 4-6: Stable drops formation without satellite droplets after ejection from the nozzles (courtesy of Mebius d.o.o.)

4.5 Description of the procedure for CCM MEA preparation by inkjet printing

The supplied Gore-Select Membrane was used according to instructions in as prepared form. The backing foil on one side was peeled off and the membrane was mounted on the heating platen of the inkjet printer. The cathode catalyst was deposited on the exposed membrane side with Pt loading of 0.2 mg/cm^2. The catalyst layer was then dried by heating the printer platen to 60 °C for 20 minutes. The membrane was dismounted from the platen, and the backing foil peeled off from the other (anode) side. The cathode side backing foil was mounted on the platen and the membrane was mounted on this backing foil so that the anode side of the membrane is available for the deposition of the anode catalyst (TEC10E50E-HT, Tanaka Kikinzoku Kogyo K.K., Japan) with Pt loading of 0.1 mg/cm^2. The anode catalyst layer was then dried after printing by again heating the printer platen to 60 °C for 15 minutes.

4.6 Post treatment of the inkjet printed CCM MEAs

The gas diffusion layers (GDL) with microporous layer (MPL) (Freudenberg Fuel Cell Products, H14C7, Freudenberg Performance Materials SE&Co.KG., Germany) are placed on the deposited catalyst ink on the anode and cathode sides, and then the entire assembly is hot pressed under vacuum. The so prepared MEAs were then packed and sent to partners for single cell testing.

5 Summary and Conclusions

5.1 Summary

While the ORR catalyst synthesis procedure remains in the frame of granted patent (JP6028027B2, US9147885B2, EP2735044B1) the subsurface catalyst nanoparticles modification is performed in line with reference [Lu B-A., 2021].
The ORR catalyst ink preparation and inkjet printing on the commercial ePTFE reinforced Nafion membrane to prepare the CCM are performed according to description provided in Section 4 of this report.
Some samples will be delivered to certain partners within the project in bare CCM form (without GDL + MPL), and some as complete MEA (with GDL+MPL, but without seal).
The single cell tests will be then accomplished by project partners and the results of these tests will be delivered to Mebius together with the analyses and comments accomplished by project partners.
In the next task Mebius will use the modified catalyst support to improve the anchoring of catalyst nanoparticles on the support. The next series of MEAs will be prepared for single cell testing at project partners.

5.2 Conclusions

In the T3.2 Mebius has prepared the ORR catalyst with subsurface modified nanoparticles. This catalyst was used to prepare the first CCMs and MEAs with commercial ePTFE Nafion membrane using inkjet printing technology.
Below we describe some risks and their mitigation pertaining to the use of inkjet printing technology for CCM and MEA preparation (production).

5.2.1 Risks identification

The ink-jet printing on the Dimatix DMP-2831 is done using the Dimatix DMC-11610 print-head and accompanying 1.5 mL cartridges. The print-heads have 16 nozzles with a diameter of 21,4 µm, and allow for printing of various fluids, including those with nano-particles of a size below 200 nm. The print-head uses a piezo-electric mechanism to produce and jet 10 pL drops onto the substrate. This limitation presents some difficulties in practice, as it is very difficult to mill and filter the catalyst into such fine powder form uniformly, without excessive losses in filtering and additional costs.
This and other factors, such as solvent drying, nozzle crusting, and material accumulating on the cleaning pad contribute to factor variance during the process of printing itself, potentially leading to nozzle clogging. This can lead to having to stop, clean, and restart the printing process, which results in lower homogeneity of the catalytic layer and effects the quantity of the catalyst deposited in the catalytic layer.
We have identified a potentially ideal solution in a larger market-available print-head Spectra 128 SL, which also requires the purchase of a printer, that can use it. In our case it will be the SUSS LP50 inkjet printer with PiXDRO technology (SÜSS MICROTEC SE, Germany). The Spectra 128 SL print-head has 128 nozzles, with a diameter of 80 µm and drop volume of 80 pl. Mebius is now in the contact with VCs to secure the investment for the purchase of necessary equipment (inkjet printer and fuel cell test station – CAPEX) and for business development, which includes growing our team and other commercialization efforts.

An additional influence on the repeatability of our MEAs is the production and precise positioning of the internal gaskets, and following that, the precise positioning of both electrodes on top of each other, both in terms of precise edge-to-edge placement, and preventing gasket slipping. At high enough production rate of MEAs (over 3000 MEAs/year), Mebius will automatize the MEAs production line.
All of the above affects the quality of the MEA after they are hot-pressed. The hot-pressing itself is an automated process.

6 Terms, Abbreviations and Definitions

MORELife	Material, Operating strategy and REliability optimisation for LIFEtime improvements in heavy duty trucks
CO	Confidential, restricted under conditions set out in Model Grant Agreement - only for members of the consortium (including the JU).
DEC	Websites, patents filing, press & media actions, videos, etc.
DEM	Demonstrator, pilot, prototype, plan designs
HW	Hardware
R	Report
OTHER	Other
PU	Public, fully open, e.g. web
WP	Work Package
PEMFC	Proton Exchange Membrane Fuel Cell
MEA	Membrane-Electrode Assembly
ICP-MS	Inductively Coupled Plasma Mass Spectrometry
RDE	Rotating Disc Electrode
TF-RDE	Thin Film Rotating Disc Electrode
XRD	X-Ray Diffraction
HRTEM	High-Resolution Transmission Electron Microscopy
STEM	Scanning/Transmission Electron Microscopy
HAADF	High Angle Annular Dark Field
HUPD	Hydrogen Underpotential Deposition
SA	Specific Activity
MA	Mass Activity
ECSA	Electrochemical Surface Area
EDS	Energy Dispersive Spectroscopy
GDL	Gas Diffusion Layer
MPL	Microporous Layer
PEM	Proton Exchange Membrane
IJP	Inkjet Printing
LDV	Light Duty Vehicle
HDV	Heavy Duty Vehicle
BoL	Beginning of Life

CCM	Catalyst Coated Membrane
AST	Accellerated Stress Test
PGM	Platinum Group Metals
SoA	State-of-the-Art
CL	Catalyst Layer
TRL	Technology Readiness Level
ORR	Oxygen Reduction Reaction
OLED	Organic Light-Emitting Diode
Oh	Ohnesorge Number
HSA	High Surface Area
We	Weber Number
Z	Inverse Ohnesorge Number
DOD	Drop-On-Demand
Re	Reynolds Number
Ca	Capillary Number
ρ	Ink Density
d	Nozzle Diameter
v	Velocity of the Ink
η	Viscosity of the Ink
γ	Surface Tension of the Ink
Wej	Jet Weber Number

Table 6-1: Terms, Abbreviations and Definitions

7 References

Reference No.	Authors; *Title*; Publication data (document reference)
[1]	Cheng-Long Yang, Li-Na Wang, Peng Yin, Jieyuan Liu, Ming-Xi Chen, Qiang-Qiang Yan, Zheng-Shu Wang, Shi-Long Xu, Sheng-Qi Chu, Chunhua Cui, Huanxin Ju, Junfa Zhu, Yue Lin, Jianglan Shui, Hai-Wei Liang, Sulfur-anchoring synthesis of platinum intermetallic nanoparticle catalysts for fuel cells, Science 374, 459–464 (2021)
[2]	Bang-An Lu, Lin-Fan Shen, Jia Liu, Qinghua Zhang, Li-Yang Wan, David J. Morris, Rui-Xiang Wang, Zhi-You Zhou, Gen Li, Tian Sheng, Lin Gu, Peng Zhang, Na Tian, and Shi-Gang Sun, Structurally Disordered Phosphorus-Doped Pt as a Highly Active Electrocatalyst for an Oxygen Reduction Reaction, ACS Catal. 2021, 11, 355−363
[3]	Seungjun Chung, Kyungjune Cho, and Takhee Lee, Recent Progress in Inkjet-Printed Thin-Film Transistors, *Adv. Sci.* **2019**, *6*, 1801445
[4]	Yuanyuan Liu and Brian Derby, Experimental study of the parameters for stable drop-on-demand inkjet performance, Phys. Fluids **31**, 032004 (2019)